Fracturing of Kimmeridge shale during heating

Alexey Yurikov[1,2], **Marina Pervukhina**[1], Maxim Lebedev[3], Valeria Shulakova[1], Yulia Uvarova[1] and David N. Dewhurst[1]

[1]CSIRO Earth Science and Resource Engineering, Perth, Australia (marina.pervukhina@csiro.au)
[2]Moscow Institute of Physics and Technology (State University), Moscow, Russia
[3]Curtin University of Technology, Perth, Australia

Abstract

Organic-rich shales, traditionally considered as source rocks, have recently become targets as unconventional reservoirs. Understanding of the initiation and development of fractures in organic-rich shales is crucially important as they drastically increase permeability of these low permeability rocks. Natural fracturing can be induced by rapid decomposition of organic matter caused by either natural heating, such as emplacement of magmatic bodies into sedimentary basins or thermal methods used for enhanced oil recovery. In this study we integrate laboratory experiments and numerical modeling to study fracture development in organic-rich shale. A cylindrical sample was heated to 330˚C and high resolution microtomographic images of the sample were obtained. Large kerogen-filled pores and cracks initiated by the heating can be identified from these images. We repeat these tests for several temperatures between 330˚C and 430˚C. The microtomographic images are processed using AVIZO to estimate the dependency between the total surface area of fractures and the temperature experienced by the sample. Total organic carbon content was also tested in the samples. This approach enables a quantitative analysis of fracture initiation and development in organic-rich shales during heating.

Key words: organic-rich shale, pyrolysis, micro-CT, TOC

Introduction

Increased interest in unconventional resources recently resulted in a large number of theoretical and experimental studies of organic-rich shales. Zargari et al. (2013) investigated elastic properties of Bakken Shale with various level of maturation on samples from different depths. The samples then underwent hydrous pyrolysis to mimic the process of natural maturation and the microstructures and local mechanical properties were compared with the same observations on the intact samples. The authors showed that the Bakken Shale becomes stronger in the process of natural maturation. i.e., the samples excavated from larger depths had larger reduced Young's moduli than the more shallow ones. The same samples locally showed lower moduli after hydrous pyrolysis as organic matter transformed to bitumen and migrated to pores. Natural fracturing is considered to to increase permeability of unconventional reservoirs (e.g., Lash and Engelder, 2005). Fractures can be induced by the pressure increase in pores caused by pyrolysis of organic matter (kerogen). Pyrolysis is the experimental process of chemical decomposition of kerogen into light hydrocarbons, namely, gas and oil.In this paper, we study fracturing of Kimmeridge organic-rich shale during heating. We present results of pyrolysis of shale samples heated to 330ºC-430ºC. We investigate the pore structure before and after heating by using high resolution microtomography.

Shale characterization and experimental procedure

The shale used in this study is Kimmeridge shale with a typical black look and density of about 1.7g/cm^3. The sample studied here has the TOC content of 23.4% which is in the range of previously reported values of 6-49 wt.%. The TOC content is also measured for the shale samples heated up to a range of temperatures and it decreases with increasing temperature of pyrolysis. The XRD study of the Kimmeridge shale shows that the rock is characterized by high carbonate content which constituted around 40 % (total percentage of calcite and dolomite) and low illite content (~6%) . Framework silicates including feldspars and quartz comprise 28%, and pyrite constitutes 1% of the total rock volume.

For studying fracture nucleation and propagation processes in shales during heating, two cylindrical samples of 5 mm height and 2 mm in diameter are prepared. The experimental procedure for each sample is as follows,(1) To visualize pre-existing fractures, the first sample is scanned using an XRadia microCT scanner with resolution of 3.5 micron;(2) The first sample is heated in OmegaLux LMF-3550 furnace from room temperature to 430ºC at a rate of 8ºC per minute. The sample is maintained under the temperature of 430 ºC for 10 minutes. Then another microtomographic image is obtained using the same microCT scanner; (3) The second sample is heated up from the room temperature to 330ºC at the rate of 8 ºC per minute and then kept at the maximal temperature for 10 minutes. The sample then is cooled down. Then a micro-tomographic image of the sample is obtained using the microCT scanner; (4) Step 3 is repeated for temperatures of 370 ºC and 390 ºC.

For better understanding of physical and chemical processes in shales during heating, the mass loss and the total organic carbon (TOC) content during heating were measured. As the samples used for the micro-CT imaging are too small for reliable measurements of the mass loss and TOC content, another four samples of the same shale were prepared and heated up to 330ºC, 370ºC, 390ºC and 430ºC. The mass of each is measured before and after heating and TOC content is measured after the heating (Table 1).

Table 1. Mass loss and TOC measurements.

#	T, ºC	Mass, g		Mass loss, %	TOC*, %
		under RT	after heating		
	20	-	-	-	30.1
1	330	0.79	0.75	5	22.9
2	370	0.96	0.89	7	19.7
3	390	0.85	0.65	24	7.9
4	430	1.18	0.83	30	0.8

Statistical analysis of fractures

Slices from each of the five microtomograms obtained for the room temperature sample, the sample heated to 330, 370 and 390 ºC and the sample heated directly to 430ºC are shown in Figure 1. These images obtained perpendicular to bedding show fracture nucleation and development as a result of heating. The intact shale (Figure 1a) exhibits a typical shale layered structure with few fractures of 2-5 pixels in width. The growth and development of fractures resulting from increased temperatures is visible at the lower end of the temperature range (Figure 1b,c). The developed fracture network is anisotropic as the fracture growth occurs parallel to the bedding plane with just few cracks developed at acute angles to bedding. At 370ºC – 390ºC, a significant increase of fracture length and fracture density is observed (Figure 1c-d), indicating rapid growth and coalescence of fractures. At the highest temperature (Figure 1e), there is only a slight difference with the image in Figure 1d. This might imply that at the temperatures higher than 390ºC, the growth of large fractures slows down and new smaller fractures start to nucleate. In order to characterize the pre-existing fractures and the fractures introduced as a result of heating of the samples, the five sets of obtained microtomograms are processed using AVIZO (Visualization Sciences Group). The detailed description of the image processing procedure can be found in Shulakova et al. (2012).

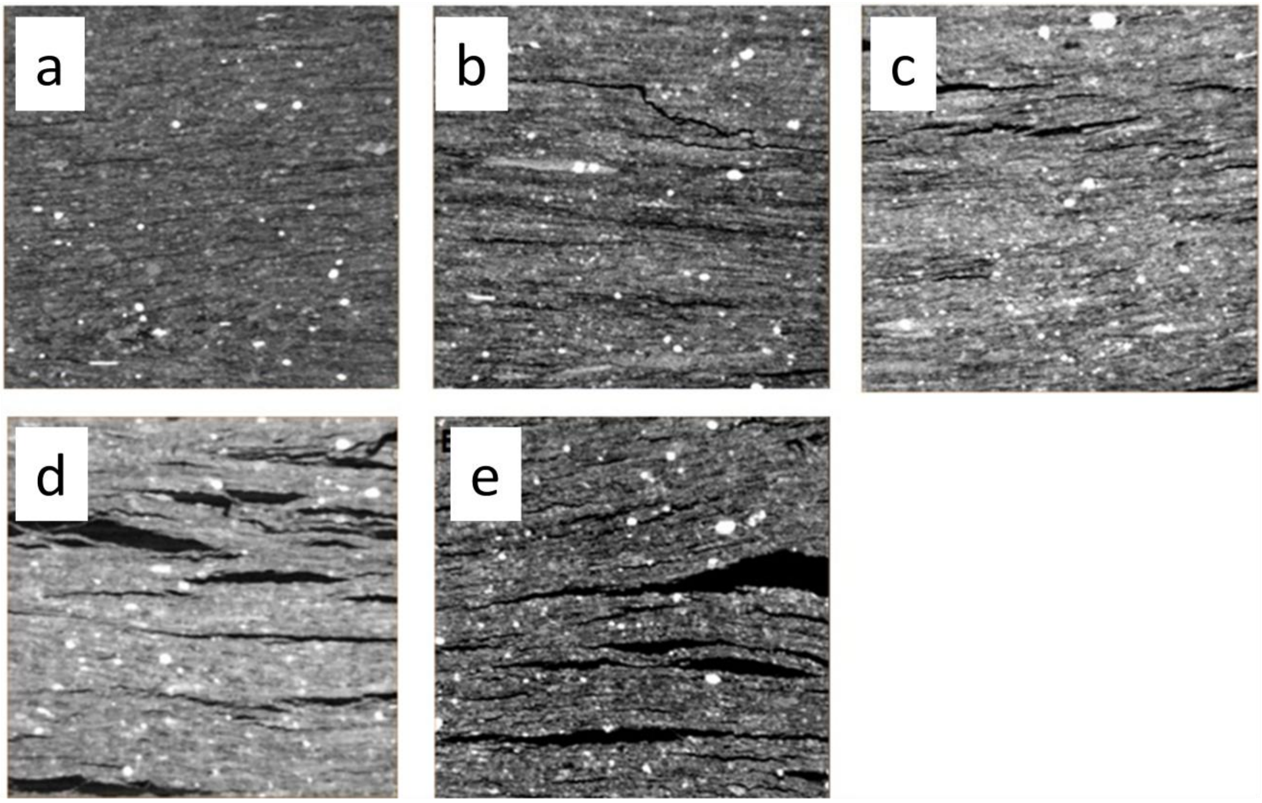

Figure 1. µCT gray scale images (400 × 400 pixels2) of shale: A) Room temperature, shale under initial conditions: tiny microcracks (2-5 pixels width) are observed. B) T = 300°C, nucleation of fractures begins. C) T = 340°C, propagation and coalescence of several fractures. D) T = 360°C, this image indicates the fast growth of fractures. E) T = 400°C, slight differences with previous slice can be observed.

The total number of fractures in the samples that experienced different maximum temperatures is shown in Figure 2b. The number of the fractures stays almost constant when the temperature increases from the 20˚C to 330 ºC. With further temperature increase, from 330 to 370 ºC and then to 390 ºC, the number of fractures normalized to the number of fractures at 20˚C drops drastically from 1 to 0.67 and 0.43, respectively. At the highest temperature, the normalized number of fractures slightly increases to 0.60. The surface areas of fractures are also analyzed for each of the samples. The results are shown in Figure 2a. One can see that with the increase of the temperature the size of the cracks increases. The number of cracks with a particular surface area decreases with increase of the surface area. The number of large fractures (with the surface area above ~40 thousand square? pixels) increases with increasing temperature. The number of small fractures (with the area of less than ~8 thousand square pixels) first decreases up to the temperature of 390ºC and then increases again in the sample that is heated up to 430ºC.

(a) (b)

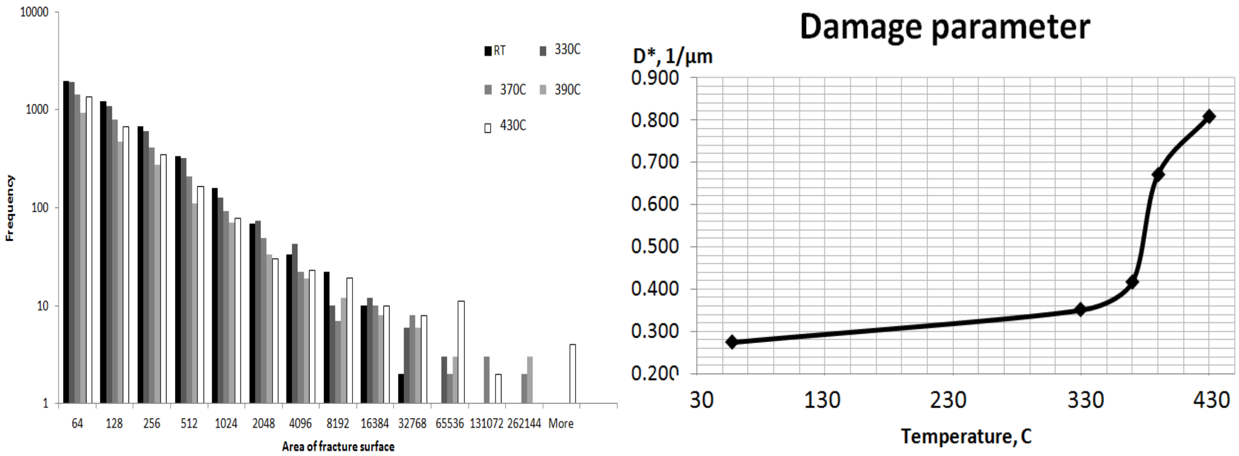

Figure 2. (a)Histogram of surface areas of fractures. (b) Dependence between damage parameter and temperature experienced by samples.

The fracture size distribution can be explained by the growth and coalescence of existing fractures and, hence, the overall number of fractures decreases. This growth also explains the decrease of the number of small fractures and the increase of the number of larger fractures. While the nucleation of new small fractures take place more slowly than the growth of the existing ones at the temperatures of 330-390 ºC, at the higher temperatures of 390-430ºC, the rapid nucleation of small fractures is initiated again along with the growth of the number of the existing cracks and the increase of the number of the large ones.

Discussion and conclusions

Total area of all fractures is presented in this work as damage parameter *D,* which is established as the total area of fractures in a unit volume (Miller et. al., 1999). The dependence between *D* and experienced temperature shows that the fastest fracture growth occurred at 370-380°C (Figure 2b). TOC and mass loss analyses show that almost all kerogen is decomposed by 430ºC (Table 1); 30% weight loss occurs after heating up to 430ºC. Most of the kerogen decomposes at 370ºC-390ºC. This is shown by slowing down of growth of total fracture area after 390ºC, the temperature dependence of the TOC content and the mass loss experiment. The obtained statistical results can be used for modeling of effects of fracture initiation and growth on elastic properties and hydraulic permeability of organic-rich shales.

References

Jin, Z.-H., Johnson, S. E., and Fan, Z. Q., 2010, Subcritical propagation and coalescence of oil-filled cracks: Getting the oil out of lowpermeability source rocks, Geophys. Res. Lett., 37, L01305, doi:10.1029/ 2009GL041576.

Lash, G. G., and Engelder, T., 2005, An analysis of horizontal microcracking during catagenesis: Example from Catskill delta complex, AAPG Bull., 89, 1433–1449, doi:10.1306/05250504141.

Miller O., Freund L.B., Needleman A., 1999, Modeling and simulation of dynamic fragmentation in brittle materials, Int. J.of Fracture, 96, 101 – 125.

Shulakova, V., Pervukhina, M., Müller, T. M., Lebedev, M., Mayo, S., Schmid, S., Golodoniuc, P., De Paula, O. B., Clennell, M. B., and Gurevich, B. 2013. Computational elastic up-scaling of sandstone on the basis of X-ray micro-tomographic images. Geophysical Prospecting 61, 287-301.

Zargari, S., Prasad, M., Mba, K. C. and Mattson, E.D., 2013, Organic maturity, elastic properties and textural characteristics of self resourcing reservoirs, Geophysics, 78(4), D223-D235